DIGITAL FILTERING ANALYSIS APPLIED TO THE ATMOSPHERE EXPLORER-C SATELLITE MESA ACCELEROMETER DATA

Joseph P. Noonan, et al

RDP, Incorporated

Prepared for:

Air Force Cambridge Research Laboratories

15 February 1975

AFCRL-TR-75-0295

DIGITAL FILTERING ANALYSIS APPLIED TO THE ATMOSPHERE EXPLORER-C SATELLITE MESA ACCELEROMETER DATA

Joseph P. Noonan, Robert W. Fioretti, and Barry Hass
RDP, Incorporated
30 Shawsheen Avenue
Bedford, Massachusetts 01730

Scientific Report Number 1

15 February 1975

AIR FORCE CAMBRIDGE RESEARCH LABORATORIES
AIR FORCE SYSTEMS COMMAND
UNITED STATES AIR FORCE
HANSCOM AFB, MASSACHUSETTS 01731

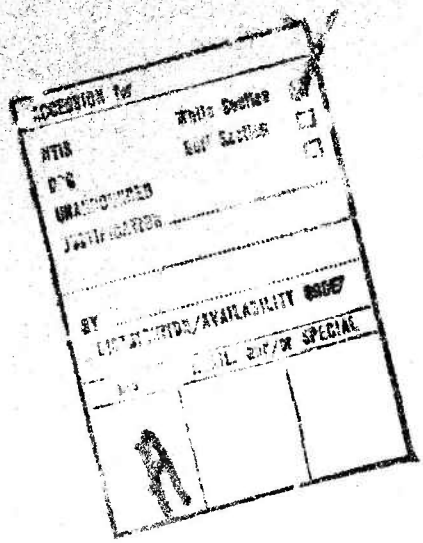

Qualified requestors may obtain additional copies from the Defense Documentation Center. All others should apply to the National Technical Information Service.

REPORT DOCUMENTATION PAGE

READ INSTRUCTIONS BEFORE COMPLETING FORM

1. REPORT NUMBER: AFCRL-TR-75-0293	2. GOVT ACCESSION NO.
3. RECIPIENT'S CATALOG NUMBER	
4. TITLE (and Subtitle): DIGITAL FILTERING ANALYSIS APPLIED TO THE ATMOSPHERE EXPLORER-C SATELLITE MESA ACCELEROMETER DATA	5. TYPE OF REPORT & PERIOD COVERED: Scientific-Interim
	6. PERFORMING ORG. REPORT NUMBER: Scientific Report No. 1
7. AUTHOR(s): Joseph P. Noonan, Robert W. Fioretti, and Barry Hass	8. CONTRACT OR GRANT NUMBER(s): F19628-73-C-0142
9. PERFORMING ORGANIZATION NAME AND ADDRESS: RDP, Incorporated, 30 Shawsheen Avenue, Bedford, Mass. 01730	10. PROGRAM ELEMENT, PROJECT, TASK AREA & WORK UNIT NUMBERS: N/A
11. CONTROLLING OFFICE NAME AND ADDRESS: Air Force Cambridge Research Laboratories, Hanscom AFB, Mass. 01731, Contract Monitor: John C. Kotelly/SUYA	12. REPORT DATE: 15 February 1975
	13. NUMBER OF PAGES: 41
14. MONITORING AGENCY NAME & ADDRESS (if different from Controlling Office)	15. SECURITY CLASS. (of this report): Unclassified
	15a. DECLASSIFICATION/DOWNGRADING SCHEDULE

16. DISTRIBUTION STATEMENT (of this Report)

Approved for public release; distribution unlimited.

17. DISTRIBUTION STATEMENT (of the abstract entered in Block 20, if different from Report)

18. SUPPLEMENTARY NOTES

19. KEY WORDS (Continue on reverse side if necessary and identify by block number)

Digital Filtering, Data Processing, Data Analysis, MESA Accelerometer, Atmosphere Explorer, Satellite, Data Reduction, Processing System, Mathematical Analysis, Accelerometer Data.

20. ABSTRACT (Continue on reverse side if necessary and identify by block number)

This report summarizes the mathematical and data analyses required to extract scientifically meaningful data from a total output signal degraded by noise. The methods described utilize digital filtering techniques, and the results are applied specifically to scientific accelerometer data flown aboard the Atmosphere Explorer satellite. Atmospheric drag and density variations are calculated utilizing these methods. The results given will be incorporated by analysts and experimenters into presentations given at scientific meetings.

DD FORM 1 JAN 73 1473 EDITION OF 1 NOV 65 IS OBSOLETE

FOREWORD

The efforts described herein were performed under contract to the Analysis and Simulation Branch (SUYA) of the Air Force Cambridge Research Laboratories (AFCRL), Hanscom Air Force Base, Bedford, Massachusetts.

TABLE OF CONTENTS

1. INTRODUCTION

The efforts described herein are part of a project to develop and implement a data processing software system for the management and analysis of data received from the AFCRL MESA (Miniature Electrostatic Accelerometer) experiment flown aboard the NASA Atmosphere Explorer (AE-C) satellite. To accomplish this task a dedicated computer system – Xerox Sigma-9 – is being utilized in a time-shared environment. Telemetry data from the fourteen major experiments aboard AE are transmitted from remote stations to NASA/GSFC, and these data are then stored on mass storage devices for use by experimenter's software. Reduced and analyzed experiment data are later restored on mass storage devices for use by all other experimenters and theoretical analysts.

The MESA Data Reduction System (DRS) which has been developed is capable of extracting raw telemetry data from the AE data base, editing and temperature-correcting the telemetry data, extracting atmospheric drag values utilizing digital filtering techniques, and calculating atmospheric density and wind data. In addition, the MESA DRS calculates Jacchia 71 model density values, lists and displays calculated parameters on printer plots and/or microfilm, and stores output data in files for on-line use by other experimenters. This system is presently being utilized in a production environment to produce reduced MESA density data on a timely basis. In addition, present plans are to modify the DRS to be capable of processing MESA data from the AE-D and AE-E satellites to be launched later in 1975.

This report will describe one segment of the MESA data reduction system, namely the digital filtering techniques used to determine atmospheric drag information from the MESA sensor outputs.

1.1 THE AE-C SATELLITE

The AE-C satellite is a sixteen (16) sided polyhedron, 53.5 inches in outside diameter, 45.0 inches high, weighing 1490 lbs., and containing 14 scientific experiments. It was launched from Vandenberg Air Force Base, California, on 16 December 1973 at 0618 GMT by a Delta vehicle into an elliptic orbit with apogee at about 4000 km, perigee at 156 km, and an inclination of 68.4 degrees.

The purpose of AE-C is to investigate the physical properties, dynamics and photochemical processes in the upper atmosphere by making closely coordinated measurements. The spacecraft differs from the usual scientific satellite in that it contains an on-board propulsion system which permits variation of perigee and apogee altitudes; in the team approach taken by investigators to analyze and compare data; in the normal spacecraft and data-taking operations; and in the concommitant rapidity with which data must be forwarded, processed and analysed.

Specifically, the AE-C mission objective is to study phenomena in the atmosphere at altitudes above 120 km. This is to be accomplished in two orbital phases: elliptic orbit and circular orbit. During the elliptic orbit phase (now completed) the spacecraft traveled in an eccentric elliptical orbit with a nominal apogee of 4000 km. and a perigee which was changed within the altitude range of 130 km. to 160 km. For the second phase, which has just begun, the spacecraft will be circularized at different altitudes, but initially between 220 km. and 240 km. In both phases the satellite's spin rate is variable, being either in the spin mode at mainly 4 rpm or in the despun mode at 1 rpo (revolution per orbit).

1.2 THE MESA EXPERIMENT

The MESA (Miniature Electrostatic Accelerometer) experiment on AE-C was designed to determine neutral atmospheric density by measuring satellite deceleration caused by aerodynamic drag. The MESA sensor consists of an electrostatically suspended proof mass which is also electrostatically rebalanced

along a sensitive axis (i.e., the longitudinal axis of the cylindrical sensor) with a force equal to the applied acceleration.

The output of the MESA is a digital pulse rate proportional to the sensed input acceleration. Vehicle dynamics, the momentum wheel, propulsion system thrusting, and instrument motions provide input "noise" accelerations. These noise accelerations are to be removed in the data analysis in order to retrieve the desired "signal" accelerations due to atmospheric drag.

This report will describe the methods used to determine atmospheric drag values from the total sensor outputs.

For a more detailed description of the AE-C satellite and the MESA experiment, see reference (2).

2. DIGITAL FILTERING ANALYSIS

2.1 GENERAL DESCRIPTION

The approach taken to extract the message signal accelerations from the total signal accelerations (that is, message signal plus noise) is provided by statistical communication theory. We can describe the acceleration data measured by MESA by the equation

$$d(t) = s(t) + n(t) \quad ,$$

where $d(t)$ = the signal received (total sensed accelerations),
$s(t)$ = the message signal (atmospheric drag),
$n(t)$ = the noise signal.

Our objective is to perform mathematical operations on $d(t)$ in order to produce a new signal, $\hat{s}(t)$, which will approximate $s(t)$ in some optimal fashion. The optimality criterion will be defined for the specific problem at hand.

2.1.1 Spectral Considerations

2.1.1.1 Fourier analysis

Arbitrary periodic functions can be represented by an infinite series of sinusoids of harmonically related frequencies. The conditions under which it is possible to write the Fourier series for a periodic function f(t) are known as the Dirichlet conditions. They require that in each period the function (a) have a finite number of discontinuities, (b) possess a finite number of maxima and minima, and (c) be absolutely convergent:

$$\int_0^T |f(t)|\, dt < \infty \ ,$$

where T is the period of f(t). If f(t) satisfies the Dirichlet conditions, we can write

$$f(t) = a_0 + \sum_{n=1}^{\infty} (a_n \cos n\omega_0 t + b_n \sin n\omega_0 t) \ ,$$

where

$$a_0 = \frac{1}{T}\int_0^T f(t)\, dt$$

$$a_n = \frac{2}{T}\int_0^T f(t) \cos n\omega_0 t\, dt$$

and

$$b_n = \frac{2}{T}\int_0^T f(t) \sin n\omega_0 t\, dt \ .$$

Since

$$\cos n\omega_0 t = \frac{1}{2}\left(e^{jn\omega_0 t} + e^{-jn\omega_0 t}\right)$$

and

$$\sin n\omega_0 t = \frac{1}{2j}\left(e^{jn\omega_0 t} - e^{-jn\omega_0 t}\right) \ ,$$

we can also write

$$f(t) = \sum_{n=-\infty}^{\infty} c_n e^{jn\omega_0 t} ,$$

where

$$c_n = \frac{1}{T}\int_0^T f(t)\, e^{-jn\omega_0 t}\, dt .$$

Note that c_n is complex and can be written as $c_n = |c_n|\, e^{j\theta n}$. Plots of $|c_n|$ and θ_n versus n are known as the line or discrete spectra of f(t) in amplitude and phase, respectively. Values of $|c_n|$ and θ_n exist only for certain values of ω, namely the fundamental frequency ω_0 and its harmonics.

Now consider a non-periodic function, g(t). The Fourier transform of g(t) is defined by

$$G(j\omega) = \int_{-\infty}^{\infty} g(t)\, e^{-j\omega t}\, dt$$

and exists if g(t) is absolutely convergent, i.e.,

$$\int_{-\infty}^{\infty} |g(t)|\, dt < \infty .$$

The inverse transform is given by

$$g(t) = \frac{1}{2\pi}\int_{-\infty}^{\infty} G(j\omega)\, e^{j\omega t}\, d\omega .$$

$G(j\omega)$ can be written as $|G(j\omega)|\, e^{j\theta(\omega)}$. $G(j\omega)$ is known as the continuous amplitude

spectrum and $\theta(\omega)$ as the continuous phase spectrum for a nonrecurring g(t). Concerning continuous spectra, we may make the following statements:

(a) The shape of the continuous amplitude and phase spectra for a nonrecurring g(t) are identical with the envelopes of the amplitude and phase line spectra for the same function recurring.

(b) All frequencies are present in the continuous amplitude spectrum in the sense that $G(j\omega)$ is defined for all ω ($-\infty < \omega < \infty$); the amplitude of any frequency component is vanishingly small, being $G(j\omega)\, d\omega/2\pi$.

Thus we see that all signals [s(t)] of interest can be represented in the frequency domain by their Fourier representation.

2.1.1.2 White noise and systematic noise

Consider a random process x(t). The autocorrelation function of the process is defined by

$$R(t_1, t_2) = E[x(t_1)\, x(t_2)] \quad .$$

The process is said to be wide sense stationary, if

(a) $E[|x(t)|^2] < \infty$ for all t

and

(b) $E[x(t_1)\, x(t_2)] = R(t_2 - t_1)$ for all t_1 and t_2 .

That is, a process is wide sense stationary if its autocorrelation function is dependent not upon the two times at which the expectation of the process is considered, but only upon the time difference, τ, where $\tau = t_2 - t_1$. Then, the autocorrelation function can be written as

$$R(\tau) = E[x(t)\, x(t + \tau)] \quad .$$

We define the power spectral density $\varphi(\omega)$ of the random process x(t) to be the Fourier transform of the autocorrelation function $R(\tau)$ of the process:

$$\varphi(\omega) = \int_{-\infty}^{\infty} R(\tau)\, e^{-j\omega\tau}\, d\tau \ .$$

It is often convenient to consider a random process x(t) with a constant spectral density N_0:

$$\varphi(\omega) = N_0 \ , \qquad -\infty < \omega < \infty \ .$$

Such a process is called white noise. It is not physically realizable since its mean squared value (power) is not finite:

$$R(0) = E[x^2(t)] = \frac{N_0}{2\pi} \int_{-\infty}^{\infty} d\omega \to \infty \ .$$

On the other hand, it often can be postulated where the actual process has an approximately constant spectral density over a frequency range much greater than the system bandwidth. For example, the thermal motion of electrons in a conducting medium give rise to broadband noise which is usually treated as being white.

Some parts of a system may also give rise to unwanted signals whose spectral density is confined to a relatively narrow section of the frequency spectrum. For example, periodic effects due to the earth's rotation will appear in certain types of ground observatory data. This is known as systematic or narrowband noise.

Narrowband noise can usually be removed from a system by the use of low pass or band pass filtering since in general the signal and noise spectra will not overlap significantly. When white noise is present, only that part of the noise

spectrum which falls outside the message bandwidth can be removed by filtering. Remember, however, that the power in the white noise spectrum is spread over its entire bandwidth, which is much wider than the signal bandwidth. Therefore, the noise power not removed by filtering will be relatively small in magnitude. Thus, the extraction of s(t) from d(t) can be viewed as a problem of frequency selection.

2.1.1.3 Optimum filters

Thus far we have seen how the problem of extracting information from noisy data can be viewed in the frequency domain as one of filtering out noise frequencies while passing that part of the total signal spectrum where the desired information lies. Because there will in general be some overlap between the message and noise spectra, a perfect filter is usually beyond our reach. The output of our filter will not be the message signal but rather an estimate of it, and we wish to construct a filter which will yield an optimal estimate. The next problem then, is to choose a criterion of optimality.

First, we define an error function E(t):

$$E(t) = |S(t) - \hat{S}(t)| \ ,$$

where $S(t)$ = the message signal, and
$\hat{S}(t)$ = the estimate of $S(t)$: the filter output.

The two most often used criteria of optimality are; (a) minimum mean squared error and (b) minimum maximum error (minimax). When using approach (a), the filter is constructed such that the mean value of $E^2(t)$ is minimized. In approach (b), the maximum value that E(t) can assume is minimized. Each has its advantages and disadvantages. The minimum mean squared error criteria will produce a filter with the smallest possible average error, but theoretically it may allow occasional relatively large deviations. On the other hand, use of the minimax criterion assures that E(t) will always be kept within known bounds.

However, the average error will be larger than that of a minimum mean squared error filter.

The choice of an optimality criterion depends on the problem at hand. For this problem the minimum mean squared error criterion was chosen, which results in a so-called matched filter. The matched filter is optimal in that it both maximized the output signal to noise ratio and can also be shown to be a maximum likelihood receiver. For these reasons it is a very important concept.

Let us define (without derivation) a matched filter for detecting a signal S(t) existing over the time interval $0 < t \leq T$ in the presence of additive white noise. The impulse response h(t) of the matched filter is given by

$$h(t) = S(t - T) \quad .$$

That is, it is the signal run backwards. Thus, we see that the output of the filter at time T is just the maximum signal energy, so that the result is intuitively pleasing.

Although not shown here, one can develop a matched filter for the case of non-white noise. In this case the filter characteristics depend on both the signal and noise structures. It basically is a function of the relation of the signal and noise frequency spectra where the filter will attempt to pass the signal band and reject the noise band as best as can be done.

For the case of baseband signals in white noise (which is perhaps the most common situation) a low pass filter with cutoff frequency determined by the signal bandwidth will closely approximate the results of the exactly matched filter. In the case considered here, where systematic noise is present as well, it is also useful to modify the filter transfer function slightly in order to assure very low gain in the frequency ranges where the systematic noise occurs. As will be shown, this is the approach which has been taken for reducing the AE data. With this background in mind, we are now prepared to discuss the design of a filter for processing telemetry data. This is done in Appendix A.

The specific characteristics of the filters chosen to process the drag data for both despun and spinning modes are described in the next section.

2.2 APPLICATION TO MESA DATA

The MESA sensors have the capability of being commanded into any of three sensitivity ranges:

Range	Full scale (g's)
A	8×10^{-3}
B	4×10^{-4}
C	2×10^{-5}

Range A was commanded for satellite thrust monitoring and was not used for density measurement. Emphasis in this report will be given to data taken from sensors in range B, since most density data were taken in this range.

2.2.1 Description of Sensed Accelerations

In order to determine how to best apply the techniques described in Section 2.1 and Appendix A to analyze MESA output data, let us first describe the in-flight accelerations sensed by the MESA instruments. These may be divided into the following – accelerations due to: (1) atmospheric drag, (2) satellite nutation, (3) momentum wheel rotation, (4) centripetal acceleration, (5) MESA instrument bias, and (6) other sensor motions.

2.2.1.1 Despun orbits

Consider first the satellite despun. In this configuration atmospheric drag information, assuming no wave motions, are sensed as zero frequency (DC) accelerations whose amplitudes vary between 10^{-8} and 5×10^{-4} g's depending upon satellite altitude. Sateilite nutation modifies the MESA output signal with a sinusoidal modulation whose frequency is 0.14 - 0.2 Hz and whose amplitude

is about 1.8×10^{-4} g's per degree of nutation on the XY sensor. Typically, nutation accelerations vary between 10^{-6} and 10^{-5} g's.

Sensor outputs are further modified by noise due to the rotation of the satellite's momentum wheel assembly (MWA). The momentum wheel rotation causes noise accelerations at high frequencies which are sensed by MESA. However, due to the telemetry data sampling rate, the modulations for the most part appear at 1.5 – 2.0 Hz. This effect is known as aliasing and is discussed in Appendix A. The amplitude of the MWA noise acceleration is about 8×10^{-6} g's.

Instrument bias causes a DC output component whose amplitude is about 1.4×10^{-6} g's. In the despun case, centripetal accelerations sensed by MESA are negligible.

Figure 1 displays a small segment of raw MESA data from the XY sensor taken on orbit 2217 at an altitude of about 170 km. Modulations on the output signal due to drag, nutation, MWA noise and instrument bias are shown.

Figure 2 illustrates raw data for the full perigee pass of orbit 2217 from all three MESA sensors. In order to attempt to measure density values at high satellite altitudes the YX sensor was in its most sensitive range (C-range). This, however, causes the YX output to saturate near perigee. Hence, for this discussion, we will consider only the XY sensor (B-range). Results of a power spectrum analysis of the XY sensor data are displayed in Figure 3 showing increased power due to (a) atmospheric drag at DC, and (b) momentum wheel and nutation noise at 1.95 Hz and 0.156 Hz, respectively. Base line data are displayed at the relative white noise level.

It is essential that the filter used to reduce these data have near 100% response at low frequencies and minimum response at those frequencies where nutation and momentum wheel noise appear; that is, that filter side-lobes be kept to a minimum. Figure 4 illustrates the filter chosen to accomplish these requirements.

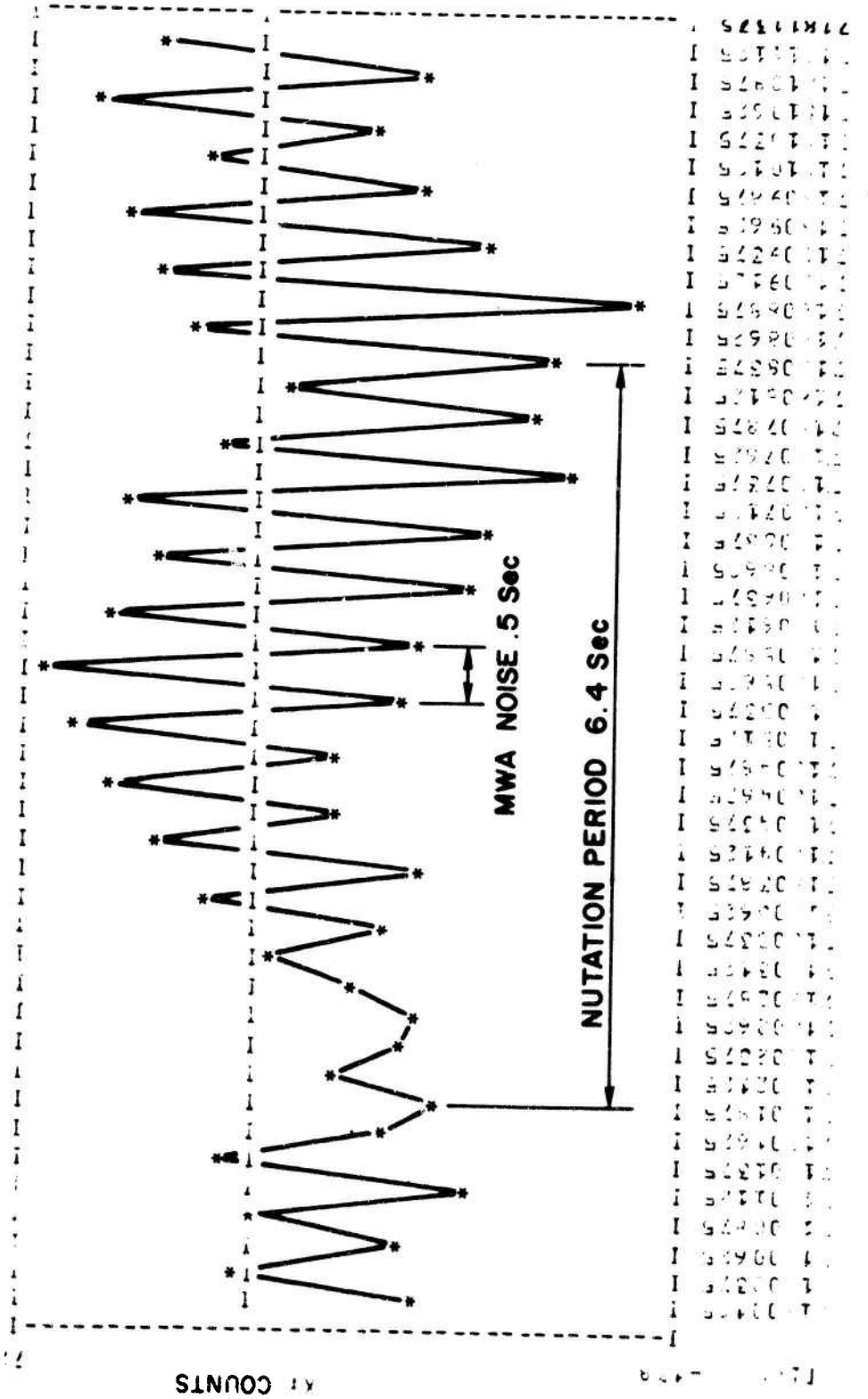

Figure 1. Raw MESA Data from XY—Sensor
Orbit 2217 Day 74180
Despun 170 KM Downleg

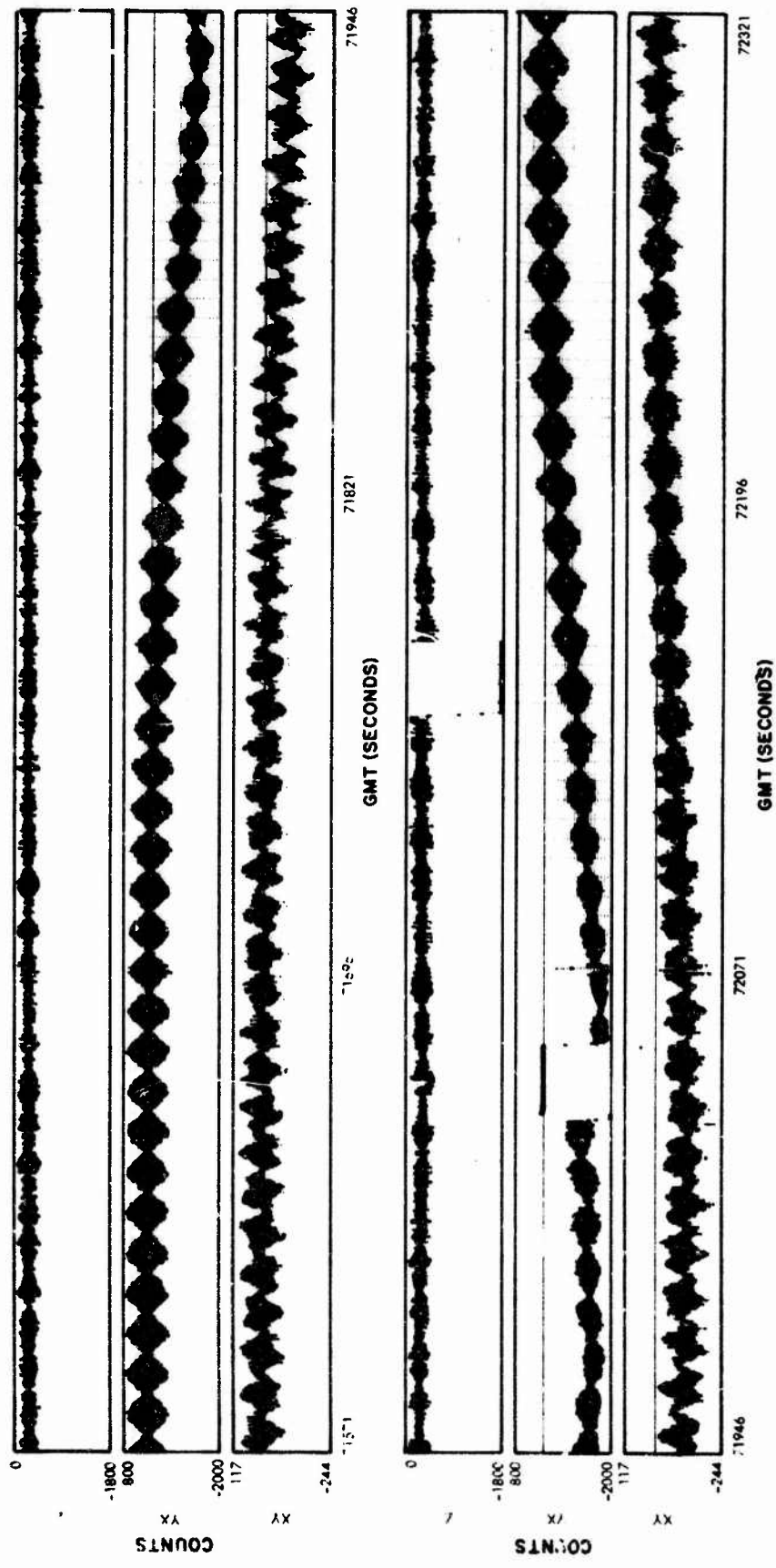

FIGURE 2. RAW MESA DATA ORBIT 2217 DAY 74180 DUSPUN

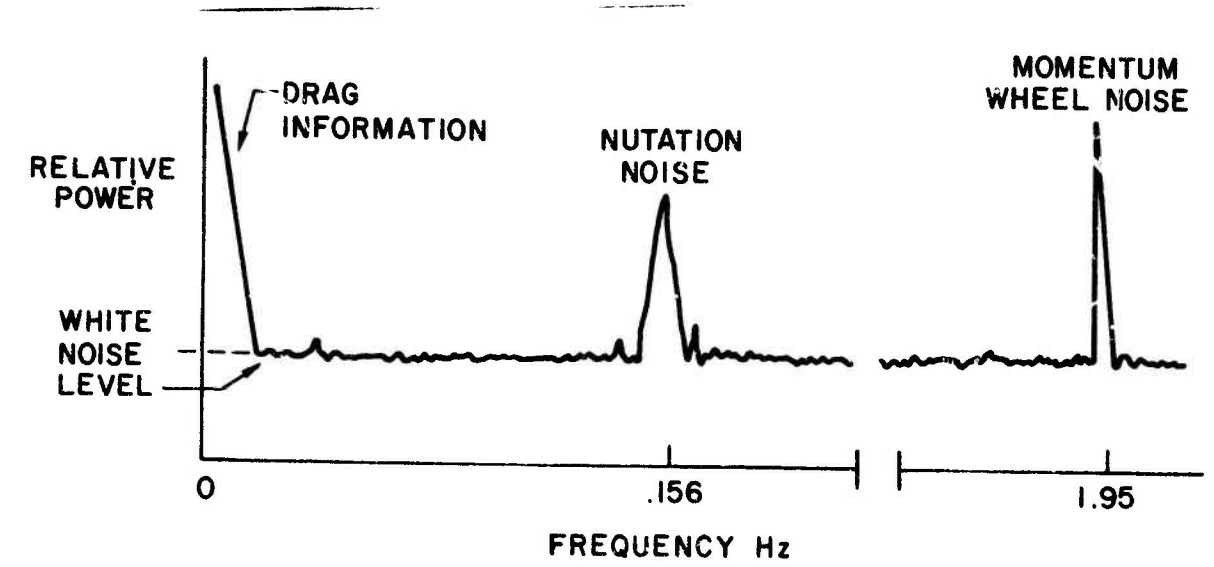

Figure 3. Power Spectrum Analysis
Orbit 2217 Day 74180

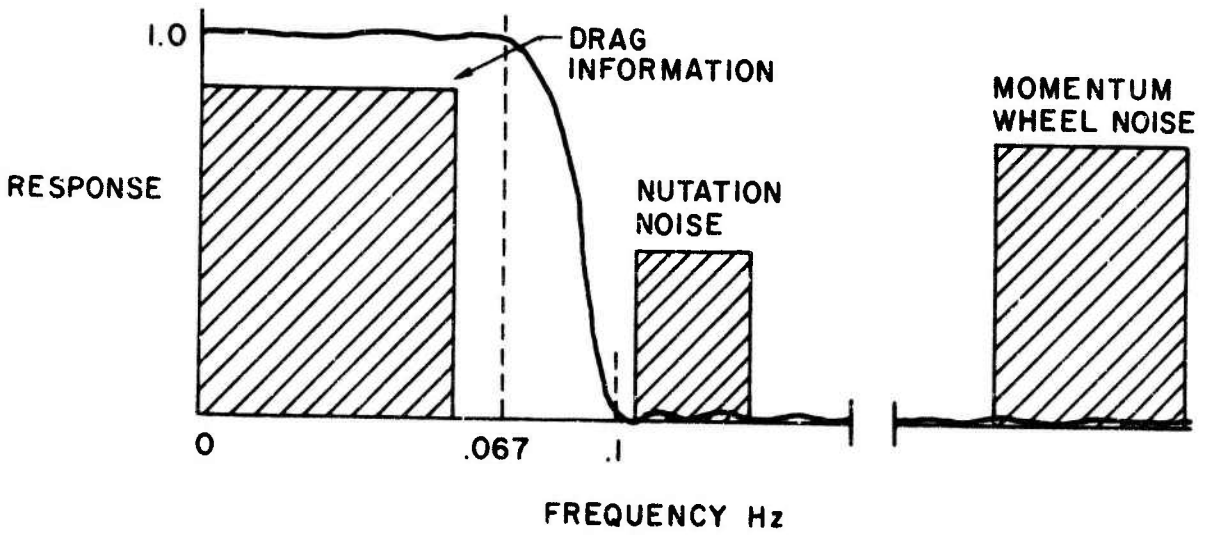

Figure 4. Filter '15 – 10' Response Curve

The filter is designated "15 - 10" because it is a low pass filter whose response is near 100% from DC to 15 seconds and is minimal from 10 seconds to .5 seconds.

Since the "15 - 10" filter chosen allows DC components to remain in the data, what remains after filtering are: (a) drag accelerations and (b) instrument bias. Bias values are removed by considering the filtered output only in those regions where atmospheric drag is negligible, that is, at high altitudes. Once bias values are determined, they are subtracted from the filtered output and the remaining values are due to atmospheric drag. Figure 5 displays MESA drag data from orbit 2217 after filtering has been done. Comparison of this with the raw outputs of Figure 2 illustrates the results of digital filtering MESA data taken on a typical despun orbit.

Atmospheric density is linearly related to drag by the following equation:

$$\rho = \frac{2MA_D}{C_D a v^2} ,$$

where ρ = atmospheric density,
M = satellite mass,
A_D = total drag acceleration,
C_D = drag coefficient,
a = satellite presentation area,
v = satellite velocity.

Final density values for orbit 2217 are shown in Figure 6.

The "15 - 10" filter allows variations of atmospheric drag at frequencies lower than 0.067 Hz to "pass through" the filter, and yet noise at higher frequencies are eliminated. This is essential if density variations due to magnetic storms, for instance, are to be studied. Figure 7 illustrates this point. Density structure is clearly seen for orbit 2283 when the magnetic activity index, Kp, was 5+.

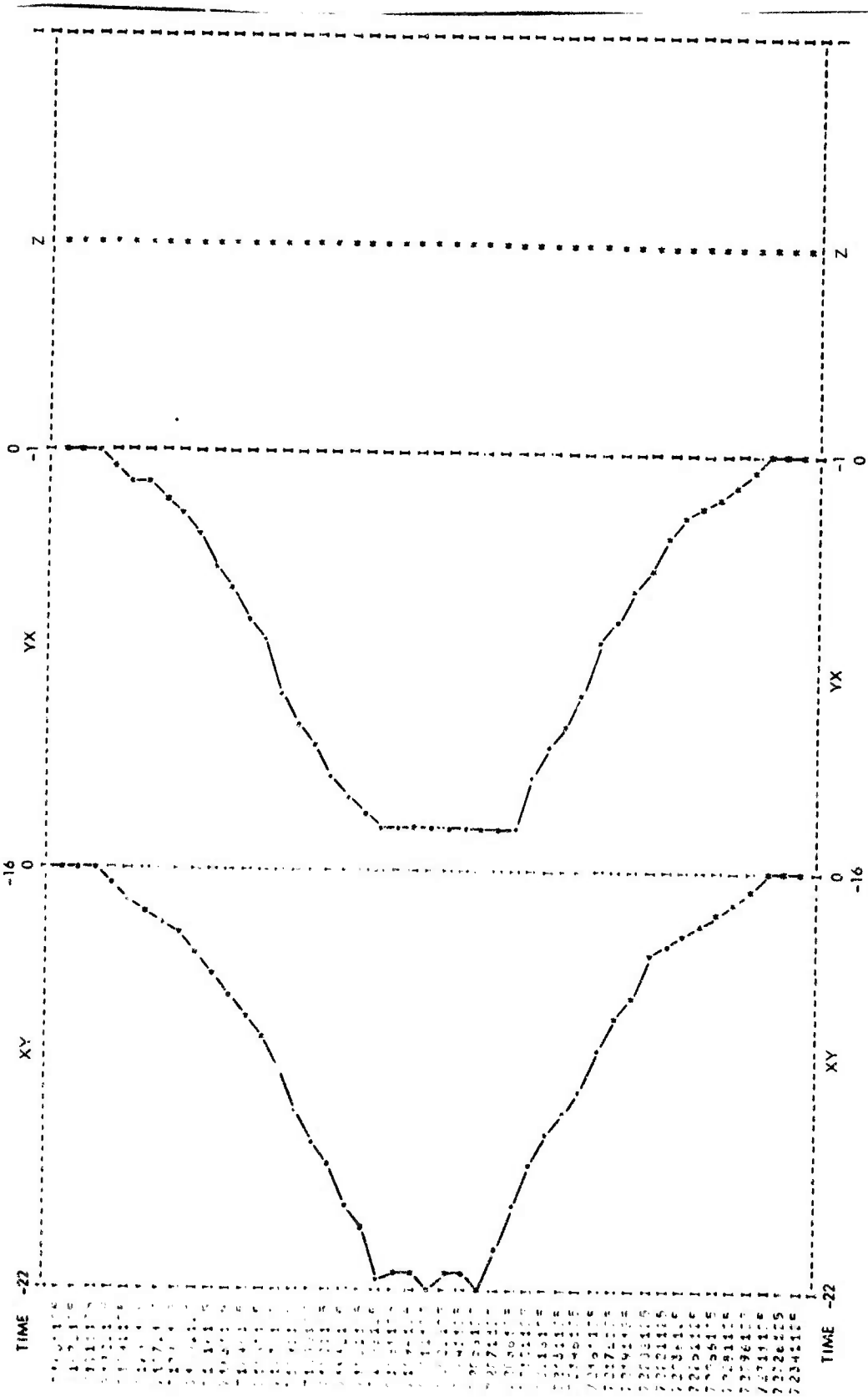

FIGURE 5. ATMOPHERIC DRAG DATA ORBIT 2217 DAY 74180 DESPUN

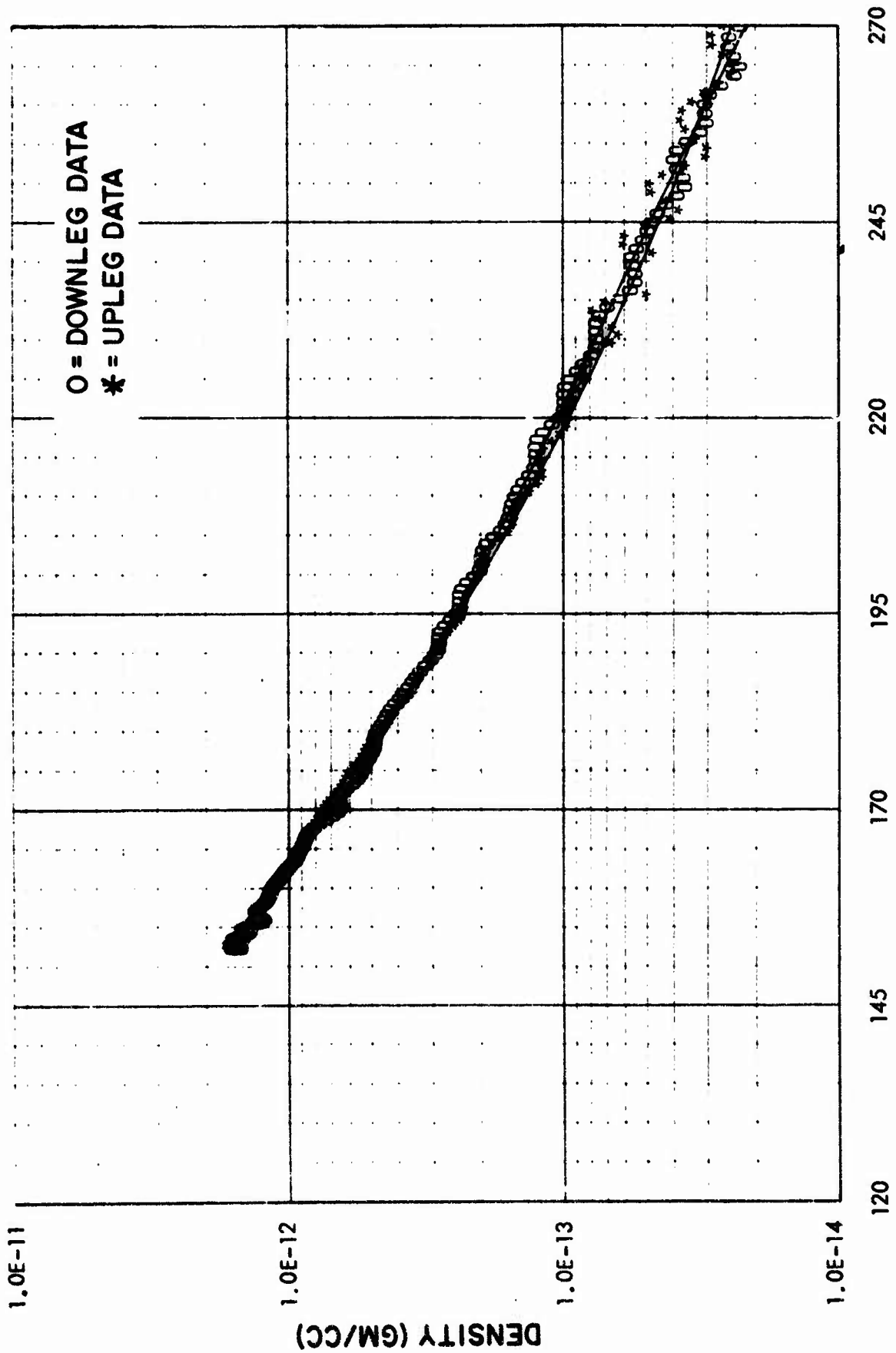

FIGURE 6. ATMOSPHERIC DENSITY DATA ORBIT 2217 DAY 74180 DESPUN

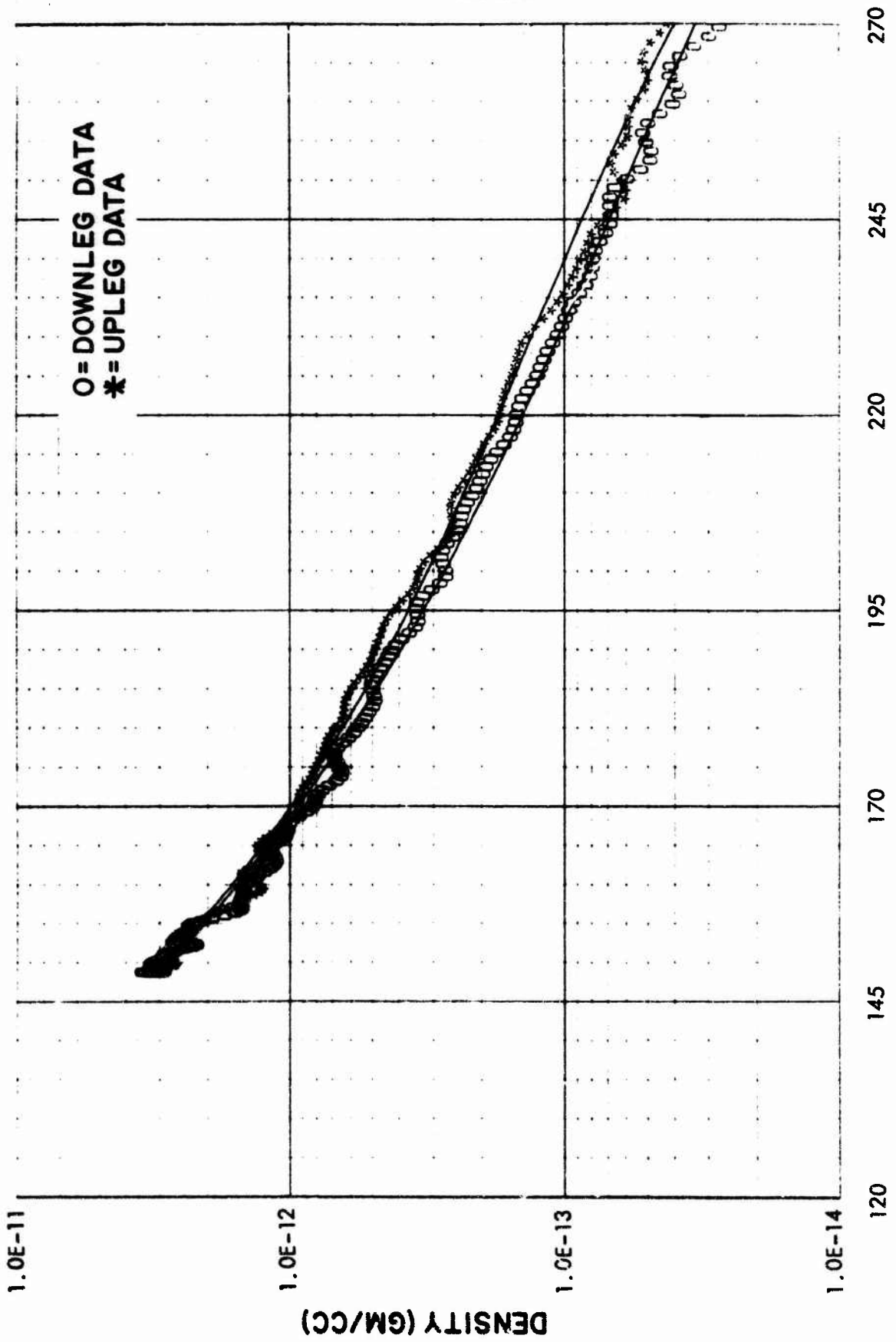

FIGURE 7. ATMOSPHERIC DENSITY DATA ORBIT 2283 DAY 74186 DESPUN

As a footnote, we have found that when the YX sensor is in its most sensitive range (C-range), noise accelerations are sensed at a frequency of about 0.067 Hz due to motions of other sensors. In this case, in order to separate these accelerations from the drag information, a "33 - 20" filter was used. The response curve of this filter is similar to the one shown in Figure 4.

2.2.1.2 Spinning orbits

We now consider the case when the satellite is spinning, nominally at 4 rpm. In this configuration, although atmospheric drag information would normally appear at low frequencies (near DC) the satellite spinning causes the drag measurements to be "chopped" at the spinning rate. Mathematically, this is equivalent to multiplying the measured drag signal by a sine wave at the spin frequency. Equivalently, the power spectrum of the drag signal is shifted in frequency to the spin frequency. This is illustrated below:

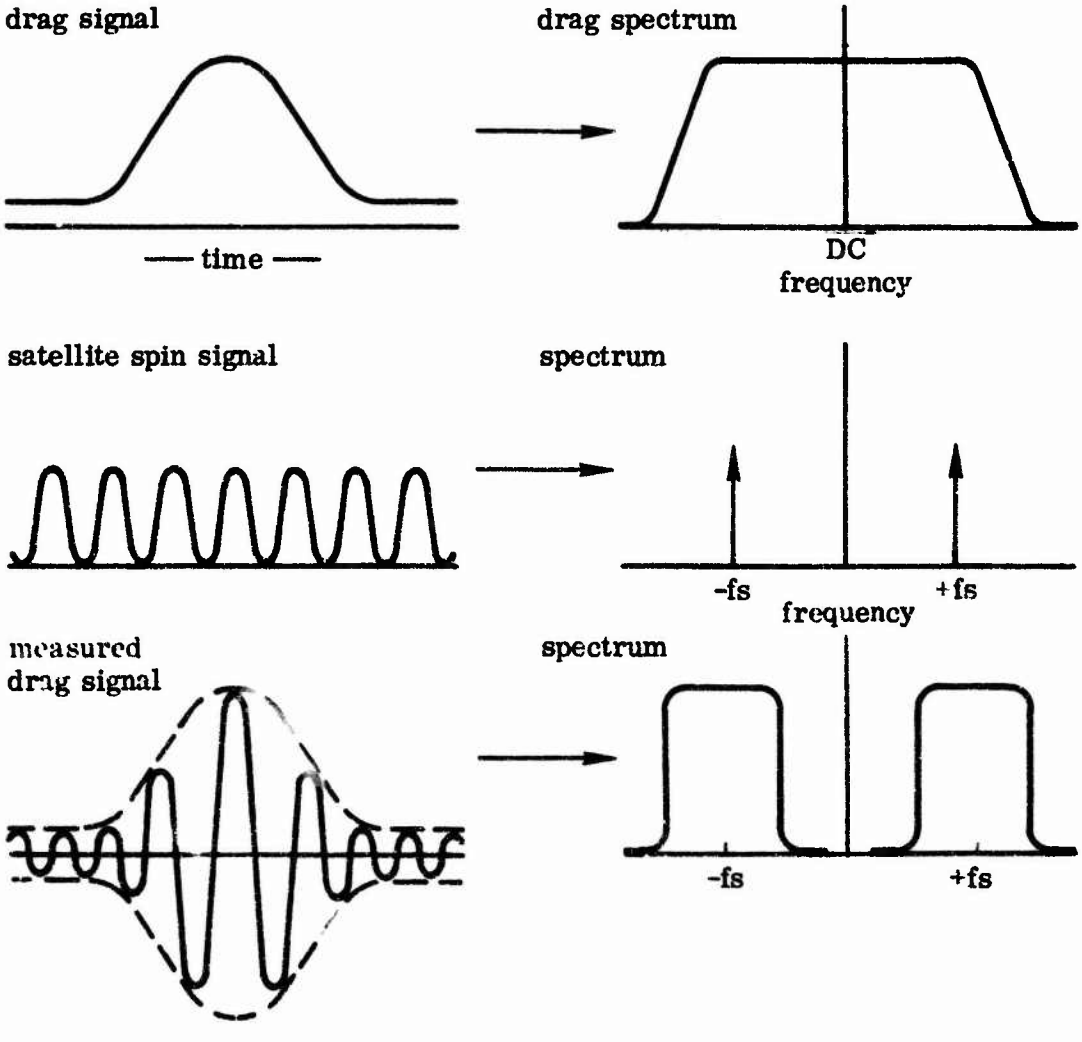

The amplitude of the drag information varies between 10^{-8} and 5×10^{-4} g's depending upon the satellite altitude. In the spinning mode the spin axis nutation modifies the MESA output as a 0.1 - 0.11 Hz sinusoid. As in the despun mode, nutation accelerations average about 1.8×10^{-4} g's, per degree of nutation on the MESA XY sensor.

Momentum wheel related accelerations for the most part again appear as high frequency modulations at 0.6 - 0.8 Hz with amplitudes averaging about 8×10^{-6} g's. In addition, accelerations due to movement of other sensors sometimes appear at frequencies lower than the spin frequency, typically about 0.033 Hz.

Figure 8 displays typical output data from MESA on orbit 2437 when the satellite was spinning at 0.067 Hz. Power spectrum analysis results from the XY sensor data are shown in Figure 9. Drag information is displayed as increased power at the spin frequency, with nutation effects and momentum wheel noise indicated.

To extract drag information from the total MESA signal in the spinning mode, a "band-pass" filter was designed with the characteristics shown in Figure 10. This filter removes (a) unwanted nutation accelerations which appear at about 0.102 Hz, (b) some motions of other instruments at about 0.033 Hz, (c) bias and centripetal accelerations appearing near DC, and (d) momentum wheel noise at 0.6 - 0.8 Hz. At the same time it is centered at 0.067 Hz to allow atmospheric drag information to pass.

The filter parameters were chosen to ensure that the filter would describe the maximum variation in atmospheric drag by passing the drag signal information, centered at the satellite spin frequency, having a bandwidth within the filter bandwidth. That is, the drag signal bandwidth is within .013 Hz of DC before modulation by the spin frequency.

The spectrum of this drag signal after spin modulation will reside within the filter bandwidth. At the same time all non-atmospheric noise accelerations at frequencies of less than 0.05 Hz and greater than 0.1 Hz will be removed by the filter.

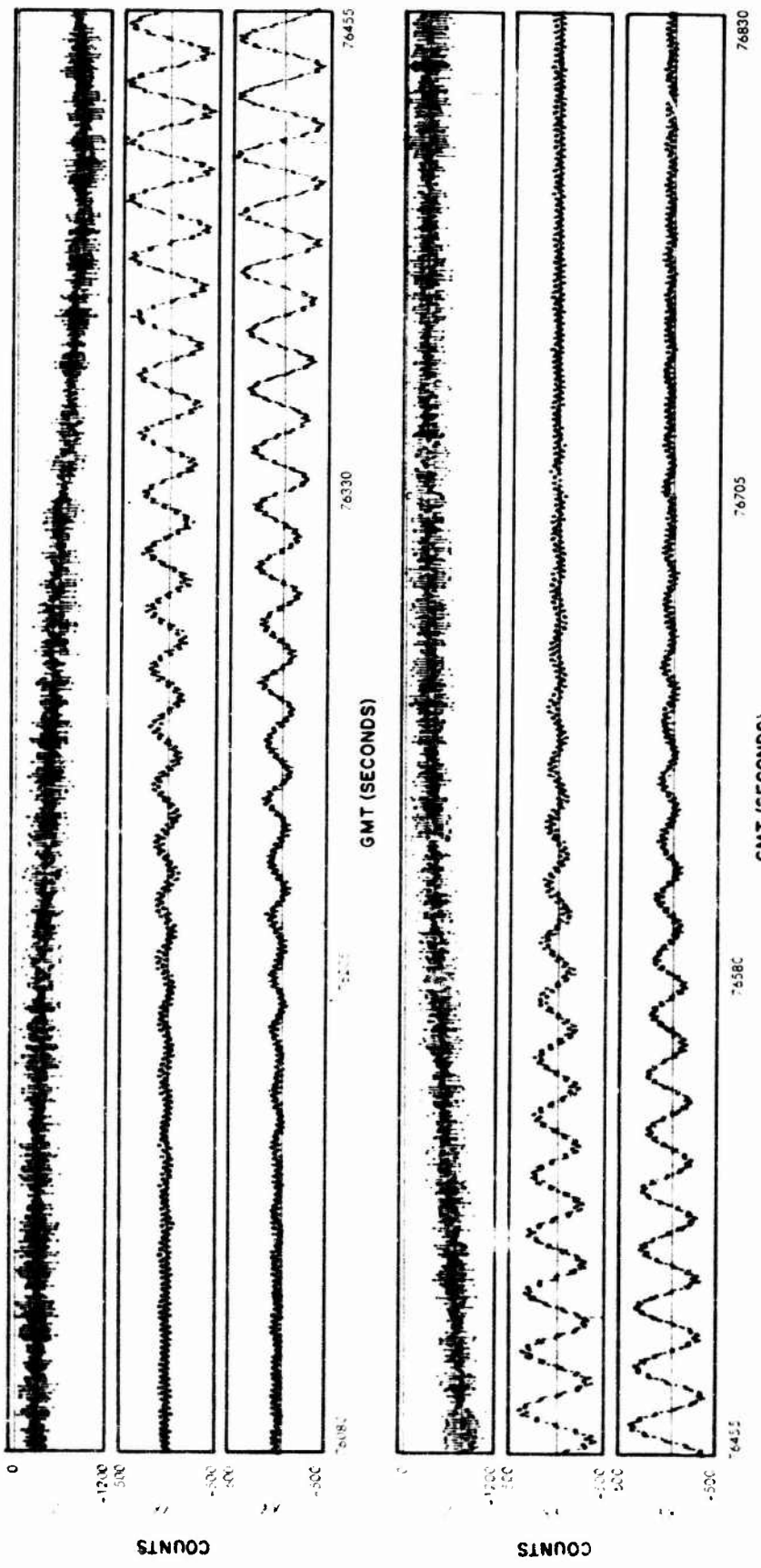

FIGURE 8. RAW MESA DATA ORBIT 2437 DAY 74198 SPINNING

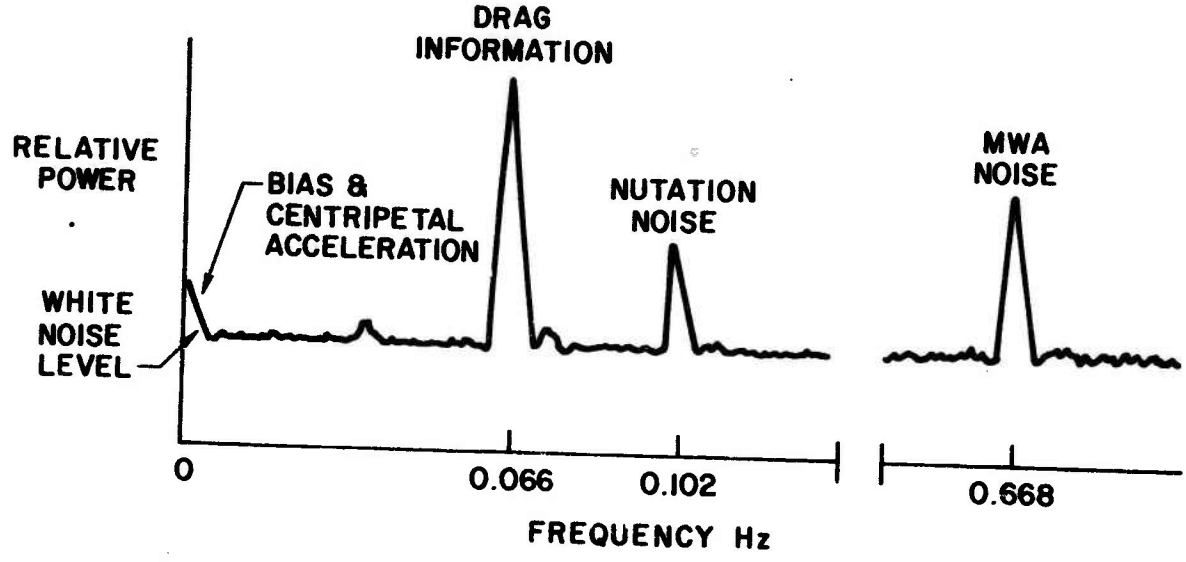

Figure 9. Power Spectrum Analysis
Orbit 2437 Day 74198

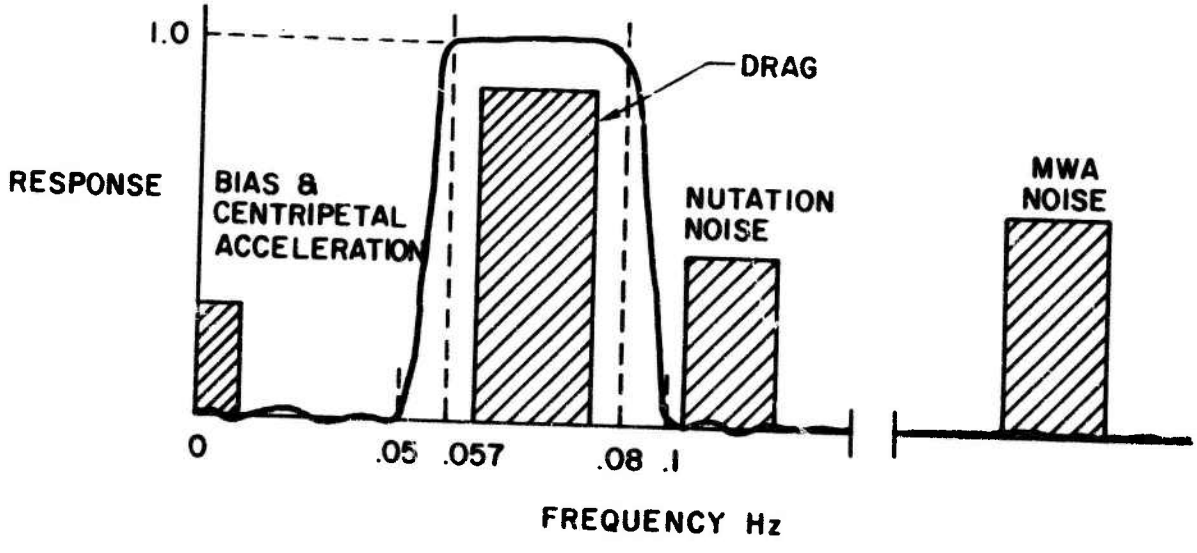

Figure 10. Band-Pass Filter

Since DC components are removed from the data by the bandpass filter (as indicated by the response curve in Figure 10), instrument bias and centripetal accelerations are filtered out and hence need not be separately removed.

Figure 11 displays MESA drag data from 2437 after filtering has been done. Comparison of this with the raw outputs of Figure 8 illustrates the results of digital filtering MESA data taken on a typical spinning orbit. Final density values for this orbit are shown in Figure 12.

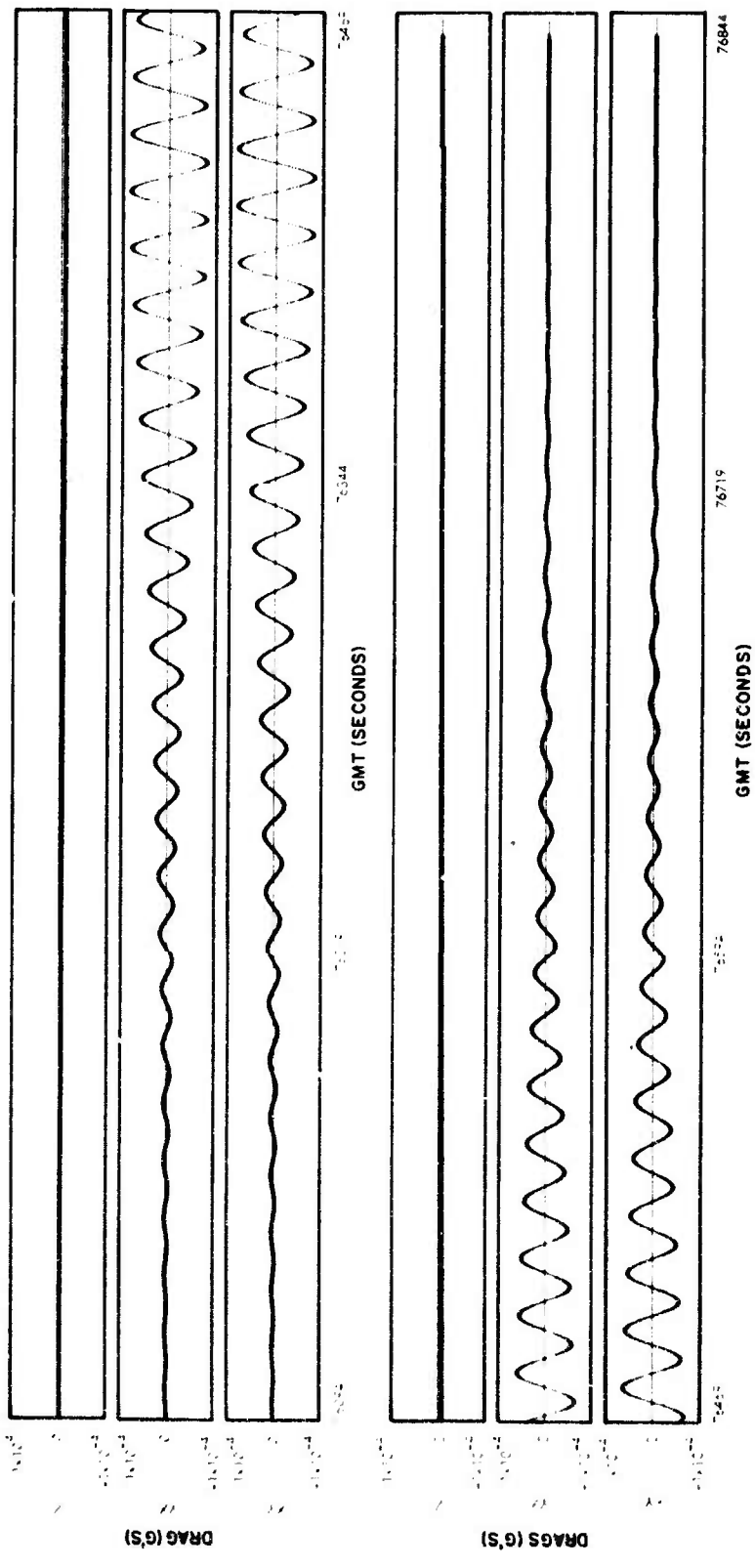

FIGURE 11. ATMOSPHERIC DRAG DATA ORBIT 2437 DAY 74198 SPINNING

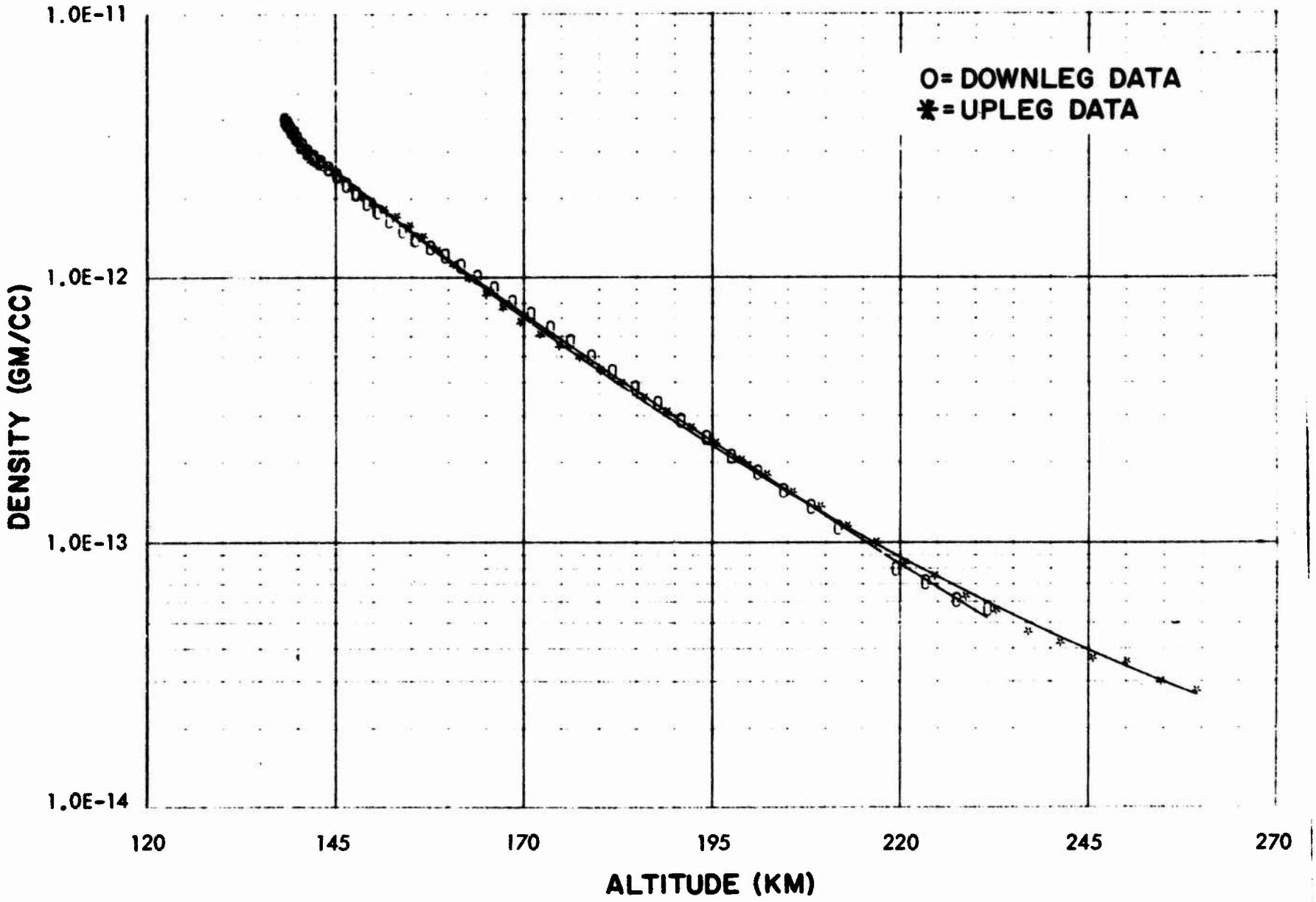

FIGURE 12. ATMOSPHERIC DENSITY DATA ORBIT 2437 DAY 74198 SPINNING

APPENDIX A

THE LEAST SQUARES APPROXIMATION FOR NON-RECURSIVE DIGITAL FILTERS

(The following treatment is taken in part from Behannon and Ness (Reference [1]).)

In general a numerical filter consists of a set of "weights" W_k which determine the actual transfer function W(f) of the filter. (The design of a numerical filter begins with establishing the shape of the data window in the frequency domain which will give the desired effect.) Having specified the theoretical transfer function, the remainder of the problem consists of determining the weights W_k in such a way that the actual transfer function, or frequency response, approximates the desired one as well as possible. A perfect low pass filter, for example, would leave unaltered all frequency components from f = 0 to the desired cutoff frequency f_L and then would suppress all frequencies greater than f_L. The response of an actual numerical filter can only approximate this ideal behavior, with the accuracy of the approximation depending on the values of various design parameters.

As in the simple smoothing process, a numerical filter is applied, such that

$$y_0(t) = \sum_{k=-M}^{N} W_k y(t + k\Delta t) \quad . \tag{1}$$

The filtering is accomplished by "sliding" the filter along the data, applying it to M + 1 + N data points to produce the filtered equivalent of the data point which has been multiplied by W_0 and then moving each weight to the next point in the series and repeating the application. Repetition of the process until all the data in a given run have been covered produces a series of filtered data points which defines the output function 0(t). Within the precision of the filter these points will trace out the input function I(t) with the unwanted high frequency components removed (if a low pass filter is being used).

As an illustration consider that the time domain representation of the smoothing process for a running mean filter is a "window" or square wave:

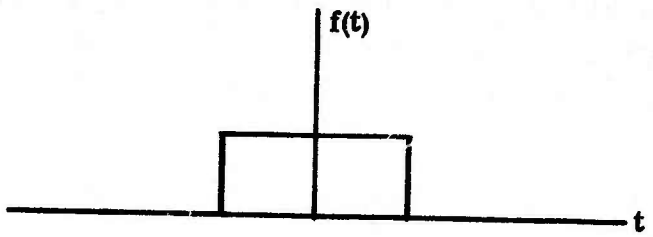

(For the sake of completeness, a derivation of the frequency domain representation of f(t) is given in Appendix B which demonstrates that a running mean filter is a form of a low pass filter.)

If the process is applied a second time, the result is f(t) convolved with itself. This results in a triangle function:

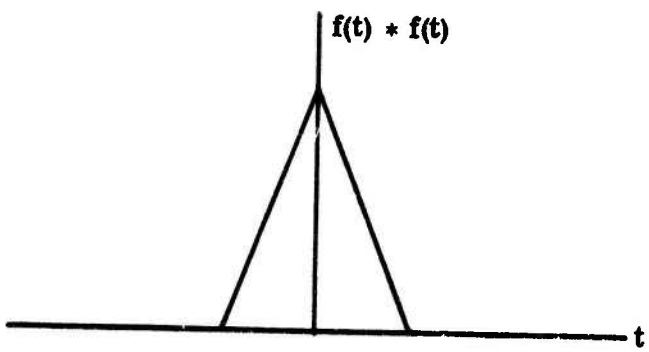

A third application will result in three parabolic segments:

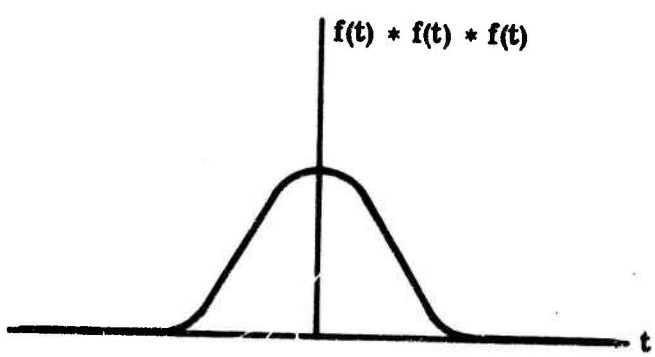

It can be seen that as the smoothing process is applied repeatedly, the time domain representation of the filter approaches a normal or Gaussian curve. One would expect this result from the Central Limit Theorem. Note also that the spectrum of a Gaussian curve is a Gaussian curve as well. Thus, the filter shape in the frequency domain will also be Gaussian.

When experimental data are derived by discretely sampling some phenomenon at equally spaced intervals of time, the problem of aliasing may occur in which the sampling rate is low enough to confuse two or more frequencies in the data. The net result is that they appear to be the same frequency. To avoid this problem and hence to define a unique input function as described by a set of data points, one must be able to assume that the phenomenon studied is spectrally limited to the range $|f| < f_c$, where $f_c = f_s/2$, f_s being the sampling frequency and f_c, being the cut-off or Nyquist frequency. If such an assumption is valid, then the function has been sampled frequently enough so that all significant frequency components are determinable. This is a result of the sampling theorem of information theory (Reference (3)). The sampling theorem states that if a function G(t) contains no frequencies higher than W cycles per second, then it is completely determined by giving its ordinates at a series of points spaced 1/2W seconds apart, the series extending throughout the entire time domain.

The problem of filter design consists of determining the M + 1 + N weights W_k such that the transfer function of the filter as defined by

$$W(p) = \sum_{k=-M}^{N} W_k \, e^{i\pi kp} \quad ,$$

where $p = f/f_c$ approximates optimally, in the least squares sense, the desired transfer function. The transfer function for a perfect filter may be written in the form

$$T(p) = G(p) \, e^{i\varphi(p)} \quad ,$$

$\varphi(p)$ being the phase shift. We shall require that the mean square deviation between T(p) and W(p) over a specified interval $-p'$ to $+p'$, given by

$$I = \frac{1}{2p'} \int_{-p'}^{p'} |T(p) - W(p)|^2 \, dp$$

be minimized by proper choice of the M + 1 + N weights W_k. It can be shown that this leads to (for the case of an Ideal Low Pass Filter)

$$W_0 = \int_0^P dp = P$$

and for $k \neq 0$

$$W_k = \frac{\sin \pi k p}{\pi k} .$$

The preceding equations may be used to compute low pass filter weights for sharp cutoff, but they lead to an approximation of the ideal transfer function which exhibits a large overshoot for values of p slightly smaller or greater than P. This is a manifestation of the Gibbs phenomenon discussed in most works on Fourier analysis. This phenomenon occurs near a discontinuity in a function which is being approximated by a finite series of size N. As N increases, the position at which the maximum occurs moves nearer to the point of discontinuity, but the value of the overshoot amplitude is independent of N. In approximating a perfect low pass filter transfer function. The deviations from the theoretical values near the cutoff frequency are usually much larger than can be allowed.

To avoid the sharp cutoff overshoot, instead of making the function zero for all values of p, it can be continued by a sine function which has the same value and the same derivative at p + P as the transfer function and, together with its derivative, becomes zero for a specified value of p. Instead of using p directly, however, it is more convenient to use a parameter h_p, of magnitude corresponding to the change in p during 1/4 cycle of the sine termination function. If the ratio of the change in p to h_p is included in the argument of the sine function, it

forces both the termination function and its derivative to have the necessary values at their end points. The geometry of the sine termination is shown in Figure A1.

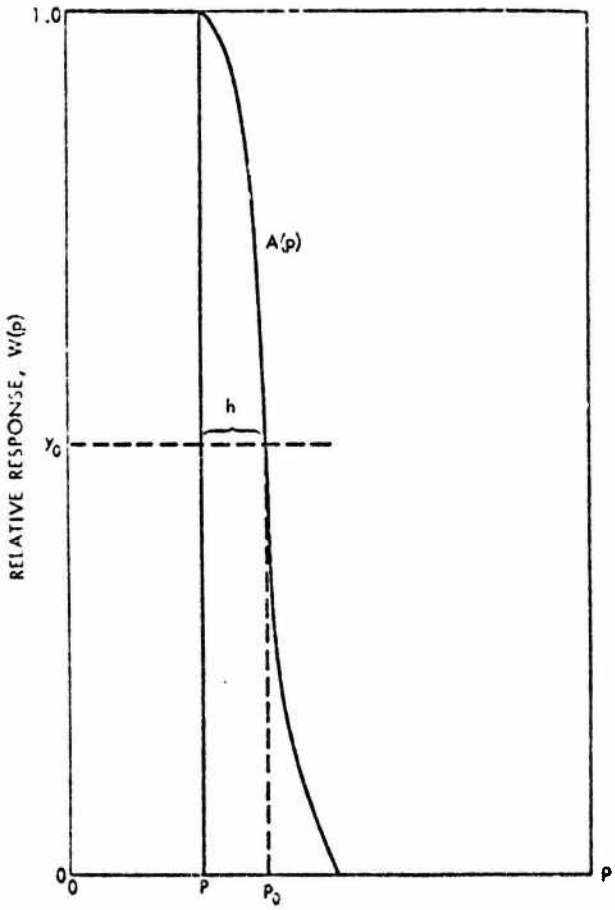

Figure A1 – Geometry of the sine termination function A(p) which is used to provide smoother cutoff for low pass filter frequency responses (Figure taken from reference (1).).

To design a filter with a sine termination, h must be as small as possible but such that the actual frequency response of the filter does not depart from the theoretical response by more than a permissible tolerance. (As h approaches zero, the filter approaches a sharp cutoff filter.) In Figure A2 we see the

improvement offered by sine-terminated filters over sharp cutoff filters designed for the same cutoff frequencies and with the same number of weights.

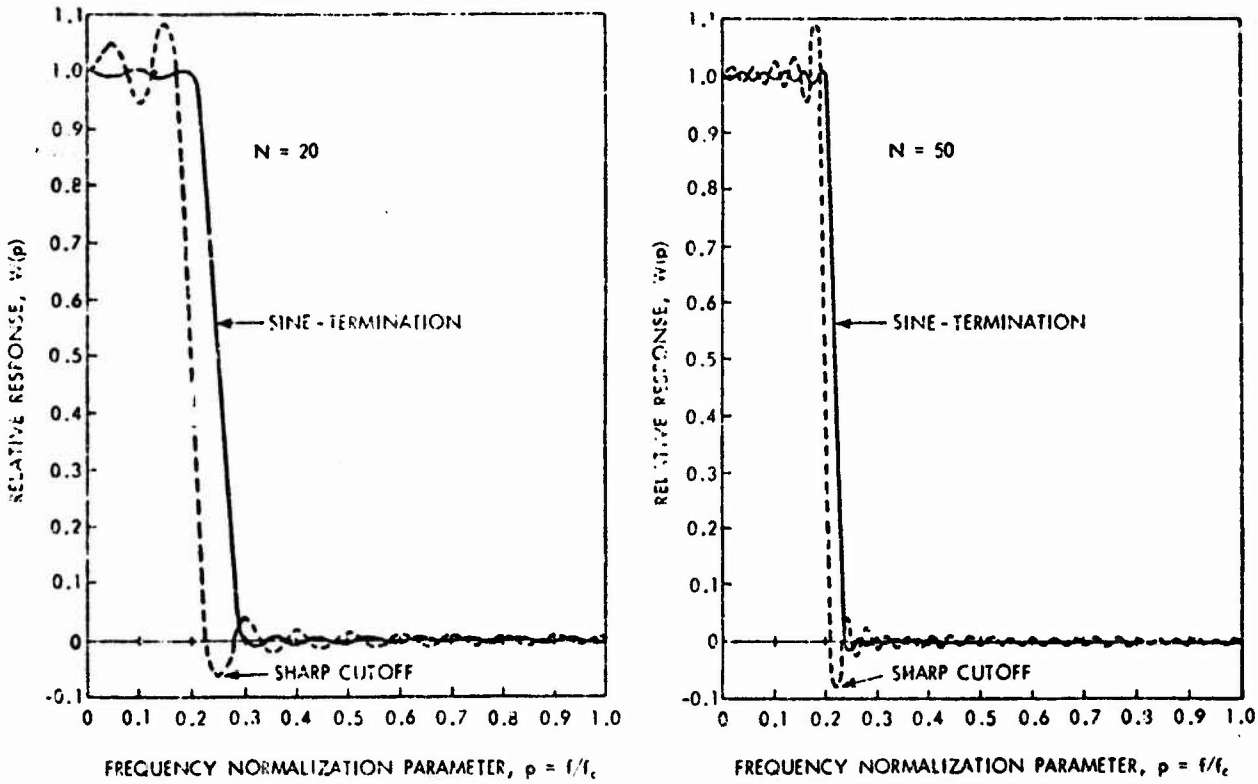

Figure A2 – Marked contrast between sharp cutoff and sine-terminated approximations to an ideal filter with low cutoff at p = 0.2 is illustrated by the frequency response of two filters with N = 20 and N = 50, respectively. The approximation is improved by use of the larger filter (Figure taken from reference (1).).

The weights for a sine-terminated filter can be shown to be $W_0 = P + h$, and

$$W_k = \left[\frac{\cos \pi kh}{1 - 4k^2h^2}\right]\left[\frac{\sin \pi k(P + h)}{\pi k}\right] .$$

One further correction may be added to the weights in order to normalize the gain to 1.0 at p = 0. Let the value of the k^{th} weight be designated by L_k. Then

$$\Delta = 1 - \left(L_0 + 2 \sum_{k=1}^{N} L_k \right)$$

and the corrected weight is given by

$$W_k = L_k + \frac{\Delta}{2N + 1} \quad .$$

Once the weights have been computed, the gain or frequency response may be found from

$$W(p) = W_0 + 2 \sum_{K=1}^{N} W_k \cos \pi kp \quad .$$

The above results are easily extended to the design of bandpass filters. That is, one obtains a bandpass filter (centered at frequency q) with the shape of a given low pass filter by simply shifting the low pass filter spectrum by $\pm q$, as illustrated below.

Low pass filter

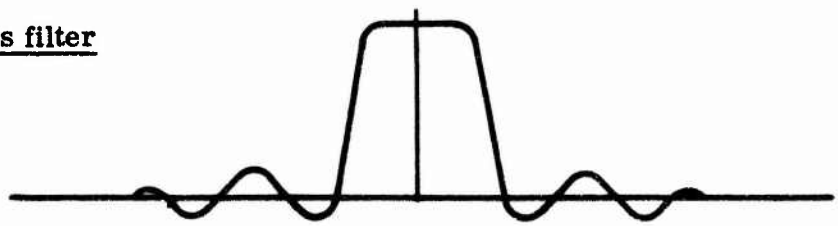

Band pass filter

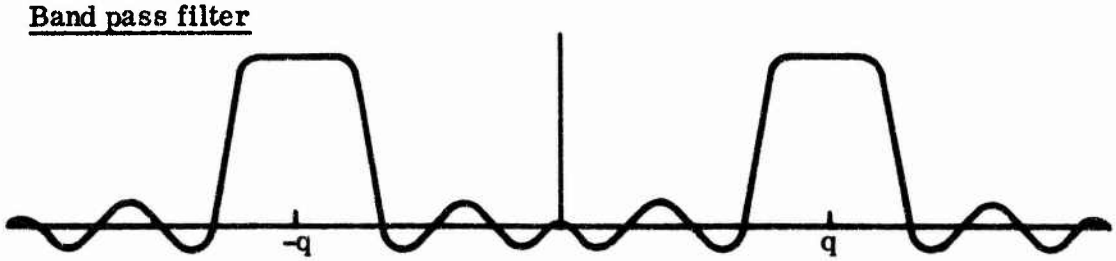

Mathematically, this is done by multiplying the low pass filter time response as shown here.

$$W^{BP}(t) = (e^{i2\pi qt} + e^{-i2\pi qt})\, W^{LP}(t)$$

$$= 2\cos 2\pi qt\, W^{LP}(t) \quad .$$

Thus, the K^{th} weight of the bandpass filter centered at f = q is given in terms of the low pass weights by

$$W_K^{BP} = 2\cos\left(\frac{\pi Kq}{fc}\right) W_K^{LP} \quad .$$

APPENDIX B

DERIVATION OF SQUARE WINDOW TRANSFER FUNCTION

f(h) = noisy input signal

g(h) = smoothed output signal

h = space between data points

N = number of data points to be averaged.

NOTE: Two assumptions are made about f(h):

(1) f(h) has a Fourier transform F(w)

(2) F(w) has no DC component, i.e., F(0) = 0.

$$g(h) = \frac{1}{N\Delta h}\int_{h-(N\Delta h/2)}^{h+(N\Delta h/2)} f(\kappa)\, dk$$

$$= \frac{1}{N\Delta h}\left\{\int_{-\infty}^{h+(N\Delta h/2)} f(k)\, dk - \int_{-\infty}^{h-(N\Delta h/2)} f(k)\, dk\right\}$$

$$= \frac{1}{N\Delta h}\{a(h) - b(h)\}$$

$$a(h) = \int_{-\infty}^{h+(N\Delta h/2)} f(k)\, dk = \int_{-\infty}^{\infty} f(k)\, u\left[\left(h + \frac{N\Delta h}{2}\right) - k\right] dk \ ,$$

where u(h) is the unit step function, thus

$$a(h) = f(h) * u\left(h + \frac{N\Delta h}{2}\right) \ ,$$

where "*" signifies convolution.

$$A(w) = F(w)\left[\frac{1}{jw} + \pi\delta(w)\right] e^{jw(N\Delta h/2)}$$

$$= F(w)\,\frac{e^{jw(N\Delta h/2)}}{jw} + \pi F(0)\,\delta(w)\,e^{jw(N\Delta h/2)}$$

$$= F(w)\,\frac{e^{jw(N\Delta h/2)}}{jw}$$

from assumption 2 above. Similarly,

$$B(w) = F(w)\,\frac{e^{-jw(N\Delta h/2)}}{jw}$$

$$G(w) = \frac{1}{N\Delta h}\,[A(w) - B(w)] = \frac{1}{N\Delta h}\,F(w)\left[\frac{e^{jw(N\Delta h/2)} - e^{-jw(N\Delta h/2)}}{jw}\right]$$

$$G(w) = F(w)\left[\frac{e^{jw(N\Delta h/2)} - e^{-jw(N\Delta h/2)}}{2j\left(\frac{WN\Delta h}{2}\right)}\right] = F(w)\,\frac{\sin\left(\frac{wN\Delta h}{2}\right)}{\left(\frac{wN\Delta h}{2}\right)}$$

$$H(w) = \frac{G(w)}{F(w)} = \frac{\sin\left(\frac{wN\Delta h}{2}\right)}{\left(\frac{WN\Delta h}{2}\right)}$$

Substituting $2\pi f = w$

$$H(f) = \frac{\sin \pi fN\Delta h}{\pi fN\Delta h}\ ;$$

$$H(f) = \text{sinc}\,(N\Delta hf)\ .$$

ACKNOWLEDGEMENTS

We wish to acknowledge the support of the MESA Data Analysis Team – Dr. K.S.W. Champion (LKB), Frank Marcos (LKB), Charlton Walter (SUYA), Robert E. McInerney (SUYA), and John C. Kotelly (SUYA) – for their evaluation and recommendations in the application of these efforts to the MESA AE data.

Computer programming support were provided by the following RDP staff members: Susan M. Ruggles, Alfred J. Bird, Jules Gilbert, Daniel J. de Clercq Zubli, and John P. Fasano. To all we offer a special thanks.

Thanks also to Mrs. Rita de Clercq Zubli, technical typist to the secretarial staff, for the fine preparation of this report.

REFERENCES

(1) Behannon, K.W. and Ness, N.F., The Design of Numerical Filters for Geomagnetic Data Analysis, NASA Technical Note, NSDS TND-3341.

(2) Champion, K.S.W. and Marcos, F.A., The Triaxial Accelerometer System on Atmosphere Explorer, Radio Science, Volume 8, Number 4, pp. 297-303, April 1973.

(3) Gold, B. and Radar, C., Digital Processing of Signals, McGraw-Hill, Inc., New York, 1969.

(4) Papoulis, A., The Fourier Integral and Its Applications, McGraw-Hill, Inc., New York, 1962